

11-2016

# Interspecies Comparison of Peptide Substrate Reporter Metabolism using Compartment-Based Modeling [post-print]

Allison Tierney

*Trinity College, Hartford Connecticut, allison.tierney@trincoll.edu*

Nhat Pham

*Trinity College, Hartford Connecticut, nhatham@trincoll.edu*

Kunwei Yang

*Trinity College, Hartford Connecticut, kunwei.yang@trincoll.edu*


Brooks Emerick

*Trinity College, Hartford Connecticut, brooks.emerick@trincoll.edu*

Michelle Kovarik

*Trinity College, Hartford Connecticut, michelle.kovarik@trincoll.edu*

Follow this and additional works at: <http://digitalrepository.trincoll.edu/facpub>

 Part of the [Biochemistry Commons](#), [Biology Commons](#), and the [Chemistry Commons](#)

---



## Interspecies Comparison of Peptide Substrate Reporter Metabolism using Compartment Based Modeling

Journal:	<i>Analytical and Bioanalytical Chemistry</i>
Manuscript ID	Draft
Type of Paper:	Research Paper
Date Submitted by the Author:	n/a
Complete List of Authors:	Tierney, Allison; Trinity College, Chemistry Pham, Nhat; Trinity College, Mathematics Yang, Kunwei; Trinity College, Chemistry Emerick, Brooks; Trinity College, Mathematics Kovarik, Michelle; Trinity College, Chemistry
Keywords:	Amino acids / Peptides, Capillary electrophoresis / Electrophoresis, Modeling, Bioanalytical methods, Biological samples, Enzymes

1  
2  
3  
4  
5  
6  
7  
8  
9  
10  
11 **Interspecies Comparison of Peptide Substrate Reporter Metabolism using**  
12  
13 **Compartment-Based Modeling**  
14  
15

16  
17 Allison J. Tierney,<sup>a</sup> Nhat Pham,<sup>b</sup> Kunwei Yang,<sup>a</sup> Brooks K. Emerick,<sup>b</sup> and

18  
19  
20 Michelle L. Kovarik<sup>a,\*</sup>  
21  
22

23  
24 <sup>a</sup>Department of Chemistry, Trinity College, 300 Summit Street, Hartford, CT 06106  
25

26  
27 <sup>b</sup>Department of Mathematics, Trinity College, 300 Summit Street, Hartford, CT 06106  
28

29  
30 \*Corresponding Author. Email: michelle.kovarik@trincoll.edu. Phone: 860-297-5275.  
31

32 Fax: 860-297-5129  
33  
34  
35  
36  
37  
38  
39  
40  
41  
42  
43  
44  
45  
46  
47  
48  
49  
50  
51  
52  
53  
54  
55  
56  
57  
58  
59  
60

## Abstract

Peptide substrate reporters are fluorescently labeled peptides that can be acted upon by one or more enzymes of interest. Peptide substrates are readily synthesized and more easily separated than full-length protein substrates; however, they are often more rapidly degraded by peptidases. As a result, peptide reporters must be made resistant to proteolysis in order to study enzymes in intact cells and lysates. This is typically achieved by optimizing the reporter sequence in a single cell type or model organism, but studies of reporter stability in a variety of organisms are needed to establish the robustness and broader utility of these molecular tools. We measured peptidase activity toward a peptide substrate reporter for protein kinase B (Akt) in *E. coli*, *D. discoideum*, and *S. cerevisiae* using capillary electrophoresis with laser-induced fluorescence (CE-LIF). Using compartment-based modeling, we determined individual rate constants for all potential peptidase reactions and explored how these rate constants differed between species. We found the reporter to be stable in *D. discoideum* ( $t_{1/2} = 82\text{-}103$  min) and *S. cerevisiae* ( $t_{1/2} = 279\text{-}314$  min), but less stable in *E. coli* ( $t_{1/2} = 21\text{-}44$  min). These data suggest that the reporter is sufficiently stable to be used for kinase assays in eukaryotic cell types while also demonstrating the potential utility of compartment-based models in peptide substrate reporter design.

## Introduction

Peptide substrate reporters are short peptides, typically 3-20 amino acids long, that can be acted on by one or more enzymes of interest [1, 2]. Peptide substrates are commonly used for activity assays in place of full-length endogenous substrates because they are easier to synthesize and separate than full-length endogenous protein substrates. For detection, peptide substrates may be tagged with fluorogenic moieties [3–5], a fluorescent label [6–10], or a FRET pair [11–13]. Reporters have been developed for many enzymes, particularly kinases [2, 4, 6, 8, 10, 12, 14–16], but also proteases [11, 13, 17–19], phosphatases [9], and others [7]. Reporter development typically starts with a peptide library, often based on the consensus sequence for an enzyme's known endogenous substrates, and proceeds through optimization of the amino acid sequence for rapid kinetics, high specificity, and stability in cells and lysates [1, 10, 16].

Stability of exogenous peptides, including substrate reporters, is an active area of research because cells express a number of cytosolic peptidases that degrade peptides into amino acids for recycling into new proteins [20]. Degradation by peptidases is not a problem for assays performed with purified kinase (or other enzyme), but resistance to degradation is a key parameter for substrates for measuring the activities of enzymes when proteases are present, such as in intact cells or cell lysates. In cells or lysates, the kinetics of reporter degradation must be appreciably slower than the kinetics of reporter reaction with the enzyme-of-interest or meaningful measurements cannot be made. Practically speaking, this usually means the half-life of the reporter in the cytoplasm or cell lysate should be at least 30 minutes or longer. In general, peptides are rapidly metabolized in the cytoplasm with half-lives ranging from < 1 min to 20 min [20]. However, degradation rates depend on peptide sequence, and a variety of design principles

1  
2  
3 have been used to render exogenous peptides resistant to degradation. Strategies include the  
4  
5 incorporation of non-native amino acids (e.g., D-amino acids or N-methylated amino acids [16,  
6  
7 21]) and protection of N-termini by bulky modifications [22, 23]. The choice of modifications  
8  
9 used to stabilize a given substrate is constrained by the substrate preferences of the enzyme-of-  
10  
11 interest but is also largely empirical. As a result, peptide substrate reporters are optimized by a  
12  
13 rather time-consuming, iterative design process, in which modifications to improve stability are  
14  
15 screened for their effect on kinetics and specificity toward the enzyme-of-interest.  
16  
17  
18  
19

20  
21  
22 To date, reporters have been developed and tested almost exclusively in mammalian cells, and  
23  
24 many reporters have been validated in only one specific human cell line or a few closely-related  
25  
26 lines. Only a few reporters are tested in non-mammalian cell types [14], and fewer still in non-  
27  
28 vertebrate or single-celled model organisms [5]. General design principles for peptide substrate  
29  
30 reporters are lacking, and few reporters have been tested across species. Ideally, a reporter  
31  
32 optimized in one organism would be widely applicable to other organisms with minimal re-  
33  
34 optimization. This is particularly important as the need for studies in non-traditional model  
35  
36 organisms becomes more apparent [24]. However, to date, there has been minimal research on  
37  
38 the transferability of peptide substrate reporters between species. Such testing should examine  
39  
40 how differences between organisms affect reporter kinetics, specificity, and stability. A  
41  
42 comparison of stability across species is prerequisite to a comparison of kinetics and specificity  
43  
44 across species because meaningful kinetic data cannot be collected if reporters are not stable in a  
45  
46 range of cell types.  
47  
48  
49  
50  
51

52  
53  
54  
55 Variation in peptidase types and activities between organisms will certainly result in differing  
56  
57  
58  
59  
60

1  
2  
3 stability of reporters between species. While all species universally express a core set of sixteen  
4  
5 peptidase families, other peptidases and peptidase families are expressed exclusively in a specific  
6  
7 kingdom. For example, the peptidase family involved in signal peptide processing is a core  
8  
9 family found in the genomes of all living organisms checked to date. In contrast, *E. coli*  
10  
11 expresses a peptidase family specifically involved in bacterial interactions with surfaces, while  
12  
13 animal cells produce peptidases required for remodeling of the extracellular matrices around  
14  
15 tissue [25]. Even within a single species, peptidase activity varies by cell type; for example,  
16  
17 peptidase activity in cancer cells and cells from rheumatoid arthritis patients differs from that of  
18  
19 healthy cells [26, 27]. As a result of this variability in peptidase expression and activity,  
20  
21 systematic comparisons of peptide half-lives and a framework for interpreting peptide  
22  
23 degradation data are needed to inform future peptide substrate reporter design and applications.  
24  
25  
26  
27  
28  
29  
30  
31

32 In this work, we compare the degradation of a peptide substrate reporter (VI-B) for protein  
33  
34 kinase B across four species from four different kingdoms, *Escherichia coli* (Bacteria),  
35  
36 *Dictyostelium discoideum* (Protozoa), *Saccharomyces cerevisiae* (Fungi), and *Homo sapiens*  
37  
38 (Animalia). These organisms are evolutionarily divergent and express widely varying peptidases.  
39  
40 These differences are reflected in varying peptidase activity toward the reporter and can be  
41  
42 quantified using compartment-based models which reveal what steps in the degradation process  
43  
44 are most important in each organism. Modeling of breakdown kinetics reveals which amino acid  
45  
46 residues and fragments are targeted by peptidases; consequently, modeling results should prove  
47  
48 useful in future optimization of peptide substrate reporters. Additionally, a more thorough  
49  
50 understanding of interspecies variation in peptidase activity is relevant to future applications of  
51  
52 other peptide-based indicators, hormones, and pro-drugs.  
53  
54  
55  
56  
57  
58  
59  
60

## Materials and Methods

**Cell culture and lysis conditions.** Overnight cultures of *Escherichia coli* K12 were grown in LB (10 g/L Bacto-tryptone, 5 g/L yeast extract, 10 g/L NaCl, pH 7.5) at 37 °C with shaking. These cultures were diluted 1:100 and grown to mid-log phase (OD 0.5) before lysis. *Dictyostelium discoideum* was obtained from the Dicty Stock Center [28] and cultured at room temperature in HL-5 pH 6.4-6.7, (14 g/L proteose peptone 3, 7 g/L yeast extract, 3.5 mM dibasic sodium phosphate, and 11 mM monobasic potassium phosphate) with shaking at 180 rpm [29]. Cells were used at a density of  $2-4 \times 10^6$ /mL. For *D. discoideum* social development experiments, cells were washed and resuspended in development buffer (5 mM sodium phosphate dibasic and 5 mM potassium phosphate monobasic, pH 6.5 with calcium chloride and magnesium chloride added to final concentrations of 10 mM and 20 mM respectively before use) at a density of  $10^7$ /mL for 2-6 h prior to lysis. *Saccharomyces cerevisiae* (ATC 4040002) was cultured at 30 °C. Shaken, liquid cultures were started in YPD (20 g/L Bacto-peptone, 10 g/L yeast extract, 20 g/L dextrose) from single colonies grown on YPD plates. These overnight cultures were diluted to OD 0.2 and grown to OD 0.4 to reach mid-log phase before lysis.

Prior to lysis, all cell types were pelleted, washed, and resuspended in phosphate buffered saline (137 mM NaCl, 2.7 mM KCl, 10 mM  $\text{Na}_2\text{HPO}_4$ , 1.8 mM  $\text{KH}_2\text{PO}_4$ , pH 7.4). For *E. coli*, 200 mL of OD 0.5 culture was washed and resuspended in 1 mL of ice-cold PBS and lysed by sonicating  $3 \times$  for 10 s at power 3-4 with 1.5-2 min on ice between cycles. For *D. discoideum* cultures,  $1.5 \times 10^7$  cells were lysed by three freeze-thaw cycles using liquid nitrogen. For *S. cerevisiae*, 50 mL of OD 0.4 culture was washed and resuspended in 1.0 mL of ice-cold PBS and mixed with 1 mL



1  
2  
3 of 0.5 mm glass beads. Cells were lysed by bead beating 5× for 10 s/cycle with 1 min on ice  
4  
5 between cycles. All of the resulting lysates were centrifuged for 5-15 min at 15,000 ×g, and the  
6  
7 supernatant was removed and stored at -80 °C for up to 10 days before use. Biological replicates  
8  
9 were prepared as described above from three separate overnight cultures of each cell type.  
10  
11

12  
13  
14  
15 **Degradation assays.** The total protein concentration of each lysate was determined using the  
16  
17 fluorescamine assay with a bovine serum albumin calibration curve [30]. Lysates were diluted  
18  
19 1:1000 in 30 mM borate buffer (pH 9), mixed in a 3:1 ratio with 3 mg/mL fluorescamine in  
20  
21 acetone, and incubated in the dark for 2 min at room temperature. Fluorescence was excited at  
22  
23 390 nm and measured at 475 nm. Based on this assay, the lysate was diluted to a final  
24  
25 concentration of 3 mg/mL in phosphate buffered saline. The reaction was started by addition of  
26  
27 the peptide substrate reporter, 6FAM-GRP-NMeArg-AFTF-NMeAla-NH<sub>2</sub>, [16] to a final  
28  
29 concentration of 1 μM. Reactions were run at the normal growth temperature of each cell type:  
30  
31 37 °C for *E. coli*, room temperature (25 °C) for *D. discoideum*, and 30 °C for *S. cerevisiae*.  
32  
33 Aliquots were removed at 15, 30, 60, 90, 120, 180, 240, 300, and 360 min after the start of the  
34  
35 reaction and heated to 95 °C for 5 min to stop the reaction. Data for HeLa and LNCap cells were  
36  
37 published previously and graciously provided by the authors [16].  
38  
39  
40  
41  
42  
43  
44  
45

46 **Capillary electrophoresis.** Samples from the lysate assays were analyzed using a PA-800 Plus  
47  
48 capillary electrophoresis instrument (Beckman Coulter). The run buffer was 100 mM borate, 15  
49  
50 mM SDS, pH 11.4 [27]. The capillary was 50 μm diameter bare silica, 21 cm effective length  
51  
52 with an applied potential of 393 V/cm. Using purified standards, we confirmed that the parent  
53  
54 peptide substrate reporter and all fluorescent N-terminal fragments were separated under these  
55  
56  
57  
58  
59  
60

1  
2  
3 conditions. Peaks were identified by their migration times and confirmed by addition of purified  
4 standards. Peak integration was performed using the 32 Karat Software (Beckman Coulter).  
5  
6  
7  
8  
9

10 **Data analysis and compartment-based modeling.** Peak areas were converted to percent of  
11 total peak area and then to concentration based on an initial peptide concentration of 1  $\mu\text{M}$ . To fit  
12 our compartment-based model to the data, we first solved Equations (1)-(5) (see below and the  
13 Electronic Supplemental Material). We then used least-squares regression to solve for the rate  
14 constants by fitting the explicit solutions to Equations (1)-(5) to the kinetic data. We fit the  
15 solutions to Equations (1)-(5) sequentially, starting with the solution to Equation (1), which  
16 could be linearized. The solutions to Equations (2)-(5) cannot be linearized, so we took a  
17 nonlinear least-squares approach for these fits using the built-in Matlab function called lsqnonlin.  
18 This built-in function uses an iterative approach that searches for a minimum in the relevant  
19 parameter space using the method of steepest descent [31]. Since this is an iterative method, an  
20 initial guess must be provided with an upper and lower bound for each rate constant. We  
21 assumed that rate constants were non-negative with an appropriate upper bound (as discussed in  
22 the Supplemental Material); however, we had no initial insight into the actual rate constant  
23 values, so we attempted fitting with many different initial values and chose the parameter set that  
24 yielded the smallest residual error. To determine a 90% confidence interval for the half-lives and  
25 initial rates, we performed bootstrapping using a Monte Carlo simulation to generate 1000  
26 synthetic data sets based on the mean and standard deviation of triplicate measurements. The  
27 method of fitting the data was selected after extensive optimization. Further details of all  
28 mathematical analyses are in the Electronic Supplemental Material.  
29  
30  
31  
32  
33  
34  
35  
36  
37  
38  
39  
40  
41  
42  
43  
44  
45  
46  
47  
48  
49  
50  
51  
52  
53  
54  
55  
56  
57  
58  
59  
60

## Results and Discussion

**Identification of the products of reporter degradation.** In this work, we studied the degradation of a peptide substrate reporter for protein kinase B (PKB or Akt) in cell lysates from *E. coli*, *D. discoideum*, and *S. cerevisiae*. This reporter, called VI-B, was previously optimized using HeLa and LNCaP cell lysates [16]. PKB is a serine/threonine kinase that plays a key role in cell proliferation, stress, response, and apoptosis [32]. Previous studies have used the reporter to measure PKB activity in individual human cells, including primary tissue samples from patients diagnosed with pancreatic cancer and rheumatoid arthritis [16, 27, 33]. Both *S. cerevisiae* and *D. discoideum* express homologs of human PKB that are important in stress response [34, 35]. This reporter could be useful in probing PKB activity in these organisms, but first it is necessary to determine whether the peptide is phosphorylated by the homologous enzymes and sufficiently resistant to degradation in these systems. In this work, we assessed the degradation resistance of the peptide in lysates from *S. cerevisiae* and *D. discoideum*. Although *E. coli* does not express a PKB/Akt homolog, we also tested the stability of the reporter in *E. coli* lysates as a more general exploration of peptidase activity toward reporter molecules in range of evolutionarily-divergent organisms.

Capillary electrophoresis with laser-induced fluorescence detection was used to separate and detect all fluorescent products of the reporter degradation reactions in cell lysates (Fig. 1 a-c). In our discussion, we call the full-length peptide reporter *R* and refer to the detectable fragments by the number of amino acid residues still attached to the N-terminal fluorescent tag; for example, *F*<sub>1</sub> refers to the one amino acid fragment 6FAM-G. The optimized run buffer was able to separate all ten peaks in under twenty minutes (Fig. 1d), although peaks for *F*<sub>3</sub>, *F*<sub>4</sub>, and *F*<sub>5</sub> were

1  
2  
3 not baseline resolved from one another. Cell lysate samples for *E. coli* included  $F_4$ ,  $F_5$ ,  $F_6$ , and  $F_7$   
4  
5 (Fig. 1a) while lysates from *D. discoideum* and *S. cerevisiae* contained  $F_5$ ,  $F_6$ ,  $F_7$ , and  $F_8$ .  
6  
7

8 Lysates from all three model organisms also included the full-length, unmodified reporter, which  
9  
10 degraded over time due to peptidase activity (Fig. 1e). Phosphorylation of the reporter was not  
11  
12 expected to occur under the experimental conditions and was not observed. For quantitation, we  
13  
14 determined the percent peak area for each peptide species, which was presumed to be  
15  
16 proportionate to the relative concentration. We assessed degradation kinetics by tracking these  
17  
18 relative concentrations across ten time points from 0 min to 360 min.  
19  
20  
21  
22  
23

24 The relative concentrations of reporter and fragments, measured as fraction of total peak area,  
25  
26 were tracked as a function of reaction time. As expected, the concentration of unmodified  
27  
28 reporter decreases over time as it is cleaved by peptidases in the lysates to form shorter  
29  
30 fragments (Fig. 2 a-c), but the rates of reporter degradation differed between the three organisms.  
31  
32 Degradation was most rapid in *E. coli* (Fig. 2a), while *S. cerevisiae* lysates showed the slowest  
33  
34 degradation (Fig. 2c). As expected for first-order kinetics, the semi-log plot of reporter  
35  
36 concentration versus time is linear with more rapid degradation corresponding to a steeper slope  
37  
38 (Fig. 2d). As the parent was degraded, the relative concentrations of the fluorescent fragments  
39  
40 increased. In both *E. coli* and *D. discoideum*,  $F_7$  is the major fragment that forms; in *S.*  
41  
42 *cerevisiae*,  $F_5$  is the main fragment. At longer time points, the relative concentrations of some  
43  
44 fragments also begin to decrease, suggesting that these fragments were further degraded by  
45  
46 peptidases. To elucidate the relative kinetics of these degradation reactions, a compartment-  
47  
48 based model was employed.  
49  
50  
51  
52  
53  
54  
55  
56  
57  
58  
59  
60

1  
2  
3 **Compartment-based modeling.** A compartment-based model or multi-compartment model is a  
4 mathematical model used to describe the transmission of materials or concentrations among  
5 different components of a physical system [36]. This method is commonly used in  
6  
7 pharmacokinetic studies and was recently applied to studies of protein turnover [37]. The value  
8 of a compartment-based model lies in its simplicity as well as the fact that it represents an  
9 underlying physical process (in this case the chemistry of peptide metabolism). Essentially, a  
10 function of interest is generated from the physical process itself rather than general trends in the  
11 data. Compartment-based modeling works well with peptide degradation since the peptide  
12 reporter breaks down into smaller fragments whose concentrations are measured. In this work,  
13 we use the model to describe the concentration of each peptide over time (Fig. 3). The model  
14 includes several assumptions: (1) that there is no source of peptide fragments except for the  
15 initial full-length reporter; (2) that there is no sink, i.e., the parent peptide and fragments do not  
16 leave the system, but are simply converted to smaller fragments; (3) that any larger peptide could  
17 be cleaved to form any smaller peptide, but that only the N-terminal fragments, which retain the  
18 6-FAM label, will be detected and (4) that the system follows first-order kinetics and all rate  
19 constants are non-negative. (A ten-fold increase in substrate concentration, tested in  
20 *Dictyostelium* lysates, resulted in a ten-fold increase in rate and comparable half-life, validating  
21 the choice of a first-order kinetic model.) These assumptions describe a closed linear system  
22 whose solutions are a linear combination of exponential functions. Similar methods have been  
23 used previously to model enzymatic reactions [38].  
24  
25  
26  
27  
28  
29  
30  
31  
32  
33  
34  
35  
36  
37  
38  
39  
40  
41  
42  
43  
44  
45  
46  
47  
48  
49  
50

51  
52  
53 The compartment-based model can be translated into a series of differential equations (Equations  
54 1-5). For example, consider Equation (3), which describes the concentration of the seven amino  
55  
56  
57  
58  
59  
60

acid long fragment ( $F_7$ ) as a function of time ( $t$ ).  $F_7$  can be formed either from the parent reporter ( $R$ ) or from the 8 amino acid long fragment ( $F_8$ ), resulting in the terms  $+k_7R$  and  $+k_{87}F_8$ , respectively, where  $k_7$  is the rate constant for formation of  $F_7$  from the full-length reporter,  $R$  is the concentration of the reporter,  $k_{87}$  is the rate constant for the formation of  $F_7$  from  $F_8$ , and  $F_8$  is the concentration of the eight amino acid fragment. These two positive terms account for the formation of  $F_7$ . The negative term,  $-(k_{76} + k_{75})F_7$ , accounts for degradation of the seven amino acid fragment to form the six amino acid fragment ( $F_6$ ) and the five amino acid fragment ( $F_5$ ). The rate constants for these two degradation reactions can be combined into a rate constant reflecting the overall disappearance of  $F_7$ , called  $k_{net,7}$ . Thus Equation (3) describe the entirety of possible reactions involving  $F_7$  that are compatible with the data (in which  $F_5$  was the smallest fragment detected).

$$\frac{dR}{dt} = -(k_8 + k_7 + k_6 + k_5)R = -k_{net,R}R \quad (1)$$

$$\frac{dF_8}{dt} = -(k_{87} + k_{86} + k_{85})F_8 + k_8R = -k_{net,8}F_8 + k_8R \quad (2)$$

$$\frac{dF_7}{dt} = -(k_{76} + k_{75})F_7 + k_{87}F_8 + k_7R = -k_{net,7}F_7 + k_{87}F_8 + k_7R \quad (3)$$

$$\frac{dF_6}{dt} = -k_{65}F_6 + k_{76}F_7 + k_{86} + k_6R \quad (4)$$

$$\frac{dF_5}{dt} = k_{65}F_6 + k_{75}F_7 + k_{85}F_8 + k_5R \quad (5)$$

Fig. 3 and Equations (1)-(5) describe the fragments and corresponding reactions observed for *D. discoideum*, *S. cerevisiae*, and the human cell lines. Qualitatively the fragmentation patterns for these cells types, which are all eukaryotic, were similar; the same fragments were observed,

1  
2  
3 albeit in different quantities, in each cell type. Many peptidases unique to multicellular  
4 organisms, including humans, are extracellular peptidases that may not be retained in  
5 cytoplasmic lysates. This may explain the qualitative similarity of the fragmentation patterns  
6 observed in the human cell lines and other eukaryotic cell types [25]. The *E. coli* lysates  
7 produced slightly different fragments:  $F_8$  was not observed, but  $F_4$  was. However, the  
8 corresponding compartment-based model (Fig. S1) has the same mathematical form as that  
9 shown in Fig. 3. This type of model is deterministic, meaning the output of the model is  
10 completely determined by the model parameters. Rate constants for each reaction were obtained  
11 by solving the differential equations and then sequentially fitting the solutions to the data using  
12 least-squares regression (Table 1). For the eukaryotic cell lysate data, minimum residuals for the  
13 fitted rate constants ranged from  $10^{-6}$ - $10^{-1}$  with typical values around  $10^{-4}$ ; minimum residuals  
14 were somewhat higher for the *E. coli* lysate data, ranging from  $10^{-3}$  to  $10^{-1}$  (Table S1).

15  
16  
17  
18  
19  
20  
21  
22  
23  
24  
25  
26  
27  
28  
29  
30  
31  
32  
33  
34 Rate constants for the degradation reactions varied widely between reactions and organisms. At  
35 one end, some very low  $k$  values ( $10^{-13}$ - $10^{-14}$ ) suggested that certain degradation steps occur so  
36 slowly as to be negligible contributors to metabolism of the reporter. For example, formation of  
37  $F_6$  from  $F_8$  in the human cells lines would be kinetically unfavorable. At the other extreme, the  
38 maximum reported rate constant of 1 was constrained by the parameters used to fit the data in  
39 MatLab. This value was only reached for one reaction, the formation of  $F_5$  from  $F_6$  in LNCaP  
40 cells. This occurred because  $F_6$  (the six amino acid fragment) was not observed in LNCaP  
41 lysates. This observation could be explained either of two ways:  $F_6$  formed but was rapidly  
42 degraded to  $F_5$  or  $F_6$  was never formed. Because  $k_6 > 0$  for the LNCaP data, the model suggests  
43 that  $F_6$  did form from the full-length reporter but was rapidly degraded to  $F_5$ . To further test this  
44  
45  
46  
47  
48  
49  
50  
51  
52  
53  
54  
55  
56  
57  
58  
59  
60

1  
2  
3 hypothesis, we fit the LNCaP data to a simplified model that assumed  $F_6$  never formed ( $k_6 = k_{86}$   
4 =  $k_{76} = 0$ ; Fig. S2). Based on qualitative assessment and minimum residuals, the more complex  
5 model (that included formation of  $F_6$ ) was a better fit to the data for  $F_7$  and a comparable fit for  
6  $R$ ,  $F_8$ , and  $F_5$  when compared to the simplified model. The model results also suggest a further  
7 test to confirm that  $F_6$  was formed and rapidly degraded. The value for  $k_{85}$  is eight orders of  
8 magnitude higher in the complex model than in the simplified model, so incubation of  $F_8$  in  
9 LNCaP lysates could provide further support for one model over the other. Excluding the  
10 proposed rapid destruction of  $F_6$  to form  $F_5$ , the highest rate constant observed was  $10^{-1}$  for the  
11 formation of  $F_5$  from  $F_7$  in LNCaP lysates. In LNCaP lysates,  $F_5$  was the dominant fragment  
12 observed, and rate constants for its formation were  $\geq 10^{-2}$  for all possible starting peptides.  
13  
14  
15  
16  
17  
18  
19  
20  
21  
22  
23  
24  
25  
26  
27  
28

29 Interestingly, some reactions indicative of carboxypeptidase activity had non-negligible rate  
30 constants. Carboxypeptidases are peptidases that cleave the final or penultimate C-terminal  
31 amino acid residues. Many carboxypeptidases function in the extracellular space, and cytosolic  
32 carboxypeptidases (CCPs) are commonly involved in removal of glutamate residues [39].  
33  
34 Perhaps for this reason, previous research reported negligible carboxypeptidase activity toward  
35 substrates in the cytosol [22]; however, recent studies have confirmed carboxypeptidase  
36 processing of peptides in the cytosol and endoplasmic reticulum [40]. In agreement with these  
37 recent findings, all eukaryotic cell lysates generated  $F_8$  by removal of the C-terminal N-  
38 methylalanine residue. Additionally, rate constants obtained by compartment-based modeling  
39 also suggested carboxypeptidase activity in *S. cerevisiae* and human cells toward shorter  
40 fragments (Table 1). In contrast, except for the formation of  $F_8$  from the full-length reporter ( $R$ ),  
41 the rate constants for removal of the C-terminal residue in *D. discoideum* lysates are all  
42  
43  
44  
45  
46  
47  
48  
49  
50  
51  
52  
53  
54  
55  
56  
57  
58  
59  
60



1  
2  
3 exceedingly low. This may reflect the fact that the *D. discoideum* genome contains only four  
4 genes expected to code for carboxypeptidases, and all are expected to be membrane-bound or  
5 extracellular [28]. Like the *D. discoideum* data, data from *E. coli* lysates showed little evidence  
6 of removal of the C-terminal amino acid; instead, rate constants for *E. coli* reflected a preference  
7 for removal of two C-terminal amino acids in a single step. For example,  $F_8$  was not observed in  
8 *E. coli*, but formation of  $F_7$  from the full-length (9 amino acid) reporter had a relatively high rate  
9 constant ( $k_7$ ). Similarly,  $k_{75}$  and  $k_{64}$  were large while single amino acid removal steps  
10 (represented by  $k_{76}$ ,  $k_{65}$ , and  $k_{54}$ ) made negligible contributions to degradation. The result is that  
11 production of  $F_4$  leveled off after ~180 min when  $F_6$  was depleted even though larger fragments  
12 were still present (Fig. 2A). The mathematical modeling agreed with and explained this  
13 particular qualitative observation and clarified in general which reactions contributed to peptide  
14 degradation.

15  
16  
17  
18  
19  
20  
21  
22  
23  
24  
25  
26  
27  
28  
29  
30  
31  
32  
33  
34 In elucidating the kinetics of individual degradation reactions, the results of the compartment-  
35 based modeling are useful in optimizing the reporter for application to specific organisms. For  
36 example, the major fragment formed during degradation of the reporter in *D. discoideum* lysates  
37 was the seven-amino acid fragment,  $F_7$ . One strategy for further stabilizing the reporter would be  
38 to replace either residue 7 or residue 8 with a non-native amino acid to reduce peptidase activity  
39 at this bond; however, residue 7 is the threonine residue that is phosphorylated by protein kinase  
40 B, and modifications at this site are likely to affect phosphorylation rates adversely.

41  
42  
43  
44  
45  
46  
47  
48  
49  
50  
51  
52  
53  
54  
55  
56  
57  
58  
59  
60  
61  
62  
63  
64  
65  
66  
67  
68  
69  
70  
71  
72  
73  
74  
75  
76  
77  
78  
79  
80  
81  
82  
83  
84  
85  
86  
87  
88  
89  
90  
91  
92  
93  
94  
95  
96  
97  
98  
99  
100  
101  
102  
103  
104  
105  
106  
107  
108  
109  
110  
111  
112  
113  
114  
115  
116  
117  
118  
119  
120  
121  
122  
123  
124  
125  
126  
127  
128  
129  
130  
131  
132  
133  
134  
135  
136  
137  
138  
139  
140  
141  
142  
143  
144  
145  
146  
147  
148  
149  
150  
151  
152  
153  
154  
155  
156  
157  
158  
159  
160  
161  
162  
163  
164  
165  
166  
167  
168  
169  
170  
171  
172  
173  
174  
175  
176  
177  
178  
179  
180  
181  
182  
183  
184  
185  
186  
187  
188  
189  
190  
191  
192  
193  
194  
195  
196  
197  
198  
199  
200  
201  
202  
203  
204  
205  
206  
207  
208  
209  
210  
211  
212  
213  
214  
215  
216  
217  
218  
219  
220  
221  
222  
223  
224  
225  
226  
227  
228  
229  
230  
231  
232  
233  
234  
235  
236  
237  
238  
239  
240  
241  
242  
243  
244  
245  
246  
247  
248  
249  
250  
251  
252  
253  
254  
255  
256  
257  
258  
259  
260  
261  
262  
263  
264  
265  
266  
267  
268  
269  
270  
271  
272  
273  
274  
275  
276  
277  
278  
279  
280  
281  
282  
283  
284  
285  
286  
287  
288  
289  
290  
291  
292  
293  
294  
295  
296  
297  
298  
299  
300  
301  
302  
303  
304  
305  
306  
307  
308  
309  
310  
311  
312  
313  
314  
315  
316  
317  
318  
319  
320  
321  
322  
323  
324  
325  
326  
327  
328  
329  
330  
331  
332  
333  
334  
335  
336  
337  
338  
339  
340  
341  
342  
343  
344  
345  
346  
347  
348  
349  
350  
351  
352  
353  
354  
355  
356  
357  
358  
359  
360  
361  
362  
363  
364  
365  
366  
367  
368  
369  
370  
371  
372  
373  
374  
375  
376  
377  
378  
379  
380  
381  
382  
383  
384  
385  
386  
387  
388  
389  
390  
391  
392  
393  
394  
395  
396  
397  
398  
399  
400  
401  
402  
403  
404  
405  
406  
407  
408  
409  
410  
411  
412  
413  
414  
415  
416  
417  
418  
419  
420  
421  
422  
423  
424  
425  
426  
427  
428  
429  
430  
431  
432  
433  
434  
435  
436  
437  
438  
439  
440  
441  
442  
443  
444  
445  
446  
447  
448  
449  
450  
451  
452  
453  
454  
455  
456  
457  
458  
459  
460  
461  
462  
463  
464  
465  
466  
467  
468  
469  
470  
471  
472  
473  
474  
475  
476  
477  
478  
479  
480  
481  
482  
483  
484  
485  
486  
487  
488  
489  
490  
491  
492  
493  
494  
495  
496  
497  
498  
499  
500  
501  
502  
503  
504  
505  
506  
507  
508  
509  
510  
511  
512  
513  
514  
515  
516  
517  
518  
519  
520  
521  
522  
523  
524  
525  
526  
527  
528  
529  
530  
531  
532  
533  
534  
535  
536  
537  
538  
539  
540  
541  
542  
543  
544  
545  
546  
547  
548  
549  
550  
551  
552  
553  
554  
555  
556  
557  
558  
559  
560  
561  
562  
563  
564  
565  
566  
567  
568  
569  
570  
571  
572  
573  
574  
575  
576  
577  
578  
579  
580  
581  
582  
583  
584  
585  
586  
587  
588  
589  
590  
591  
592  
593  
594  
595  
596  
597  
598  
599  
600  
601  
602  
603  
604  
605  
606  
607  
608  
609  
610  
611  
612  
613  
614  
615  
616  
617  
618  
619  
620  
621  
622  
623  
624  
625  
626  
627  
628  
629  
630  
631  
632  
633  
634  
635  
636  
637  
638  
639  
640  
641  
642  
643  
644  
645  
646  
647  
648  
649  
650  
651  
652  
653  
654  
655  
656  
657  
658  
659  
660  
661  
662  
663  
664  
665  
666  
667  
668  
669  
670  
671  
672  
673  
674  
675  
676  
677  
678  
679  
680  
681  
682  
683  
684  
685  
686  
687  
688  
689  
690  
691  
692  
693  
694  
695  
696  
697  
698  
699  
700  
701  
702  
703  
704  
705  
706  
707  
708  
709  
710  
711  
712  
713  
714  
715  
716  
717  
718  
719  
720  
721  
722  
723  
724  
725  
726  
727  
728  
729  
730  
731  
732  
733  
734  
735  
736  
737  
738  
739  
740  
741  
742  
743  
744  
745  
746  
747  
748  
749  
750  
751  
752  
753  
754  
755  
756  
757  
758  
759  
760  
761  
762  
763  
764  
765  
766  
767  
768  
769  
770  
771  
772  
773  
774  
775  
776  
777  
778  
779  
780  
781  
782  
783  
784  
785  
786  
787  
788  
789  
790  
791  
792  
793  
794  
795  
796  
797  
798  
799  
800  
801  
802  
803  
804  
805  
806  
807  
808  
809  
810  
811  
812  
813  
814  
815  
816  
817  
818  
819  
820  
821  
822  
823  
824  
825  
826  
827  
828  
829  
830  
831  
832  
833  
834  
835  
836  
837  
838  
839  
840  
841  
842  
843  
844  
845  
846  
847  
848  
849  
850  
851  
852  
853  
854  
855  
856  
857  
858  
859  
860  
861  
862  
863  
864  
865  
866  
867  
868  
869  
870  
871  
872  
873  
874  
875  
876  
877  
878  
879  
880  
881  
882  
883  
884  
885  
886  
887  
888  
889  
890  
891  
892  
893  
894  
895  
896  
897  
898  
899  
900  
901  
902  
903  
904  
905  
906  
907  
908  
909  
910  
911  
912  
913  
914  
915  
916  
917  
918  
919  
920  
921  
922  
923  
924  
925  
926  
927  
928  
929  
930  
931  
932  
933  
934  
935  
936  
937  
938  
939  
940  
941  
942  
943  
944  
945  
946  
947  
948  
949  
950  
951  
952  
953  
954  
955  
956  
957  
958  
959  
960  
961  
962  
963  
964  
965  
966  
967  
968  
969  
970  
971  
972  
973  
974  
975  
976  
977  
978  
979  
980  
981  
982  
983  
984  
985  
986  
987  
988  
989  
990  
991  
992  
993  
994  
995  
996  
997  
998  
999  
1000

Compartment-based modeling revealed that the formation of this fragment from the full length peptide ( $R$ ) was kinetically more favorable than formation of  $F_7$  from  $F_8$  (i.e.,  $k_7 \gg k_{87}$ ). This suggests that the eight-amino acid fragment,  $F_8$ , would be more resistant to this degradation step

1  
2  
3 than the full-length reporter *R*. In this case, it would be useful to evaluate the activity of the *D.*  
4  
5 *discoideum* PKB homolog toward  $F_8$  to determine whether the fragment could be more stable  
6  
7 substitute for the full-length peptide. In yeast and human cells, the magnitudes of the rate  
8  
9 constants are reversed (i.e.,  $k_7 < k_{87}$ ), so the same strategy would be ineffective.  
10  
11  
12  
13  
14

15 **Interspecies variation in reporter metabolism.** To assess the overall degradation resistance of  
16  
17 the reporter, the value of  $k_{\text{net,R}}$  was used to calculate half-life of the reporter and the initial rate of  
18  
19 its destruction in each cell type. These values varied widely between cell types, as did more  
20  
21 qualitative measures of peptidase activity, such as the major fragment observed during the first  
22  
23 hour of degradation (Table 2). The range of initial degradation rates reported here spans two  
24  
25 orders of magnitude and is generally comparable to previous reports, which have identified  
26  
27 degradation rates of  $0.02\text{-}3 \text{ pmol mg}^{-1} \text{ s}^{-1}$  for this peptide reporter and others in lysates and intact  
28  
29 cells [23, 27, 33].  
30  
31  
32  
33  
34  
35  
36  
37  
38  
39  
40  
41  
42  
43  
44  
45  
46  
47  
48  
49  
50  
51  
52  
53  
54  
55  
56  
57  
58  
59  
60

We considered whether the differences in rates corresponded to each cell type's demand for amino acids to generate new proteins. Cytosolic peptidase activity is required for recycling of amino acids into new proteins; however, differences in degradation rate between cell types were not correlated to cell proliferation rates or proliferation rates normalized to cell volume. For example, *D. discoideum* and HeLa cells are similarly sized, but *D. discoideum* cells double in cell density every 8-12 h [29], while HeLa cells double every 15-30 h [41]. Despite the more rapid proliferation of *D. discoideum* compared to HeLa cells, the two cell types showed remarkably similar overall half-lives for the reporter (Table 2). *E. coli* and *S. cerevisiae* are smaller than these cells, but also proliferate more rapidly. Based on doubling times and cell

1  
2  
3 volumes, we estimate that *E. coli* cells generate 0.01-0.25  $\mu\text{m}^3$  of cytoplasm per minute,  
4  
5 compared to 0.1-2.3  $\mu\text{m}^3/\text{min}$  for *S. cerevisiae*, and 0.3-5.6  $\mu\text{m}^3/\text{min}$  for HeLa cells. These rates  
6  
7 are wide, overlapping, and uncorrelated with the half-lives observed for the reporter, suggesting  
8  
9 that for this particular peptide sequence degradation rates do not reflect general rates of amino  
10  
11 acid recycling. This possibility is further supported by our observation that resuspending *D.*  
12  
13 *discoideum* cultures in nutrient-free phosphate buffer (to initiate the organism's social life cycle)  
14  
15 did not enhance reporter degradation in these lysates (Table S3). Instead, the degradation rate is  
16  
17 likely constrained by the activity of specific peptidases in each organism that find the amino acid  
18  
19 sequence of the reporter or fragment to be a suitable substrate. This suggests that certain peptide  
20  
21 stabilization strategies may be more effective in certain cell types, depending on the specific  
22  
23 peptidases responsible for processing the reporter.  
24  
25  
26  
27  
28  
29  
30  
31

32 Qualitative differences in degradation showed similar interspecies variation. For the eukaryotic  
33  
34 cells, the terminal fragment (i.e., the smallest one observed) was the five amino acid fragment,  
35  
36  $F_5$ . Formation of the smaller  $F_4$  fragment would have required cleavage of the peptide bond at  
37  
38 the non-native N-methylarginine. In general, peptidase preferences skew toward small, aliphatic  
39  
40 residues at the scissile bond with particularly strong preference for the amino acid at the N-  
41  
42 terminal side of the scissile bond [42]. As a result, the basic, non-native N-methylarginine  
43  
44 residue is likely to stabilize the  $F_5$  fragment. Only *E. coli* lysates showed activity toward the N-  
45  
46 methylarginine-alanine bond and formation of  $F_4$ . *E. coli* cells express peptidases from 19  
47  
48 families that are not found in the other three cell types tested [25]. Of these 19 families, most are  
49  
50 characterized by substrate preferences that do not match that of the bond cleaved to form  $F_4$ .  
51  
52  
53 However, the endopeptidase omptin prefers a basic residue on the N-terminal side of the scissile  
54  
55  
56  
57  
58  
59  
60

1  
2  
3 bond and a non-basic residue on the C-terminal side [43]. This peptidase is expressed by *E. coli*  
4  
5 but not *D. discoideum*, *S. cerevisiae*, or human cells. These observations suggest that  
6  
7 N-methylarginine substitution may be broadly protective of the peptide bonds in eukaryotic  
8  
9 organisms, but further studies with a variety of peptide sequences are needed to confirm this.  
10  
11  
12  
13

## 14 15 **Conclusions**

16  
17 The genomes of these organisms vary widely in their capacity to express peptidases. Human  
18  
19 cells encode for a total of 745 peptidases from 77 peptidase families, compared to 92 peptidases  
20  
21 and 44 families in *S. cerevisiae*, 166 peptidases and 59 families in *D. discoideum*, and 89  
22  
23 peptidases and 48 families in *E. coli*. Hierarchical cluster analysis of the peptidase genes from  
24  
25 these species and many other organisms demonstrates that there exists a core group of peptidases  
26  
27 expressed by all cells, as well as clusters of peptidases specific to prokaryotes, eukaryotes, fungi,  
28  
29 and metazoans [25]. The cell types investigated here correspond to one organism from each of  
30  
31 these groups. As a result, we expect that these data should be representative of how the reporter  
32  
33 would be degraded in a wide range of organisms. Although degradation in LNCaP lysates is very  
34  
35 rapid for this reporter, in general, the degradation resistance of VI-B suggests that it is  
36  
37 sufficiently stable for application across the eukaryotic kingdom. This is important since the  
38  
39 PI3K-PKB pathway is well-conserved throughout eukaryotic cell types; however, further  
40  
41 research is needed to determine whether the reporter is a suitable substrate for phosphorylation  
42  
43 by PKB homologs in other species. While *E. coli* cells do not express a PKB homolog,  
44  
45 prokaryotic organisms do use their own serine/threonine kinase signaling pathways [44], and  
46  
47 these results could inform design of reporters for bacterial kinases. Additionally, bacterial  
48  
49 pathogens often disrupt eukaryotic signaling, including the PI3K-PKB pathway, during infection  
50  
51  
52  
53  
54  
55  
56  
57  
58  
59  
60

1  
2  
3 [45]. Consequently, this reporter could be applied to samples that exhibit some prokaryotic  
4  
5  
6  
7  
8  
9  
10  
11  
12  
13  
14  
15  
16  
17  
18  
19  
20  
21  
22  
23  
24  
25  
26  
27  
28  
29  
30  
31  
32  
33  
34  
35  
36  
37  
38  
39  
40  
41  
42  
43  
44  
45  
46  
47  
48  
49  
50  
51  
52  
53  
54  
55  
56  
57  
58  
59  
60

[45]. Consequently, this reporter could be applied to samples that exhibit some prokaryotic peptidase activity. More generally, these results suggest the utility of compartment-based models for optimizing substrate reporters for degradation resistance. Compartment-based modeling of degradation of several substrates with disparate amino acid sequences in many cell types will yield generalizable design principles that should speed future reporter design. Additionally, a more complete understanding of peptide metabolism in cells will be useful in the design of other peptide-based tools, including hormones and pro-drugs.

**Electronic Supplemental Material.** Additional details about the compartment-based modeling, including the model used for the *E. coli* data and minimum residuals for all rate constants, may be found in the electronic supplemental material.

**Acknowledgments.** The authors thank the Allbritton Laboratory at the University of North Carolina for generously providing advice and peptide standards, particularly Angela Proctor and Emilie Mainz for helpful discussions and their collaborator Qunzhao Wang for synthesis of the peptides. We also thank Jeremiah Marden and the Graf Laboratory at the University of Connecticut for assistance with the *S. cerevisiae* and *E. coli* cultures and lysis. This work was supported by Trinity College.

**Conflict of Interest.** The authors declare that they have no conflict of interest.

**References**

- 1  
2  
3 1. Hardie DG (2000) Peptide Assay of Protein Kinases and Use of Variant Peptides to  
4 Determine Recognition Motifs. In: Walker J, Keyse S (eds) Stress Response. Humana  
5 Press, pp 191–201  
6  
7
- 8  
9 2. Wu D, Sylvester JE, Parker LL, Zhou G, Kron SJ (2010) Peptide reporters of kinase  
10 activity in whole cell lysates. *Biopolymers* 94:475–486. doi: 10.1002/bip.21401  
11  
12
- 13 3. Yaron A, Carmel A, Katchalski-Katzir E (1979) Intramolecularly quenched fluorogenic  
14 substrates for hydrolytic enzymes. *Analytical Biochemistry* 95:228–235. doi:  
15 10.1016/0003-2697(79)90210-0  
16  
17
- 18 4. Shults MD, Imperiali B (2003) Versatile Fluorescence Probes of Protein Kinase Activity. *J*  
19 *Am Chem Soc* 125:14248–14249. doi: 10.1021/ja0380502  
20  
21
- 22 5. Kraft M, Radke D, Wieland GD, Zipfel PF, Horn U (2007) A fluorogenic substrate as  
23 quantitative in vivo reporter to determine protein expression and folding of tobacco etch  
24 virus protease in *Escherichia coli*. *Protein Expr Purif* 52:478–484. doi:  
25 10.1016/j.pep.2006.10.019  
26  
27
- 28 6. Chen C-A, Yeh R-H, Lawrence DS (2002) Design and Synthesis of a Fluorescent Reporter  
29 of Protein Kinase Activity. *J Am Chem Soc* 124:3840–3841. doi: 10.1021/ja017530v  
30  
31
- 32 7. Arkhipov SN, Berezovski M, Jitkova J, Krylov SN (2005) Chemical cytometry for  
33 monitoring metabolism of a Ras-mimicking substrate in single cells. *Cytometry* 63A:41–47.  
34 doi: 10.1002/cyto.a.20100  
35  
36
- 37 8. Wang Q, Cahill SM, Blumenstein M, Lawrence DS (2006) Self-Reporting Fluorescent  
38 Substrates of Protein Tyrosine Kinases. *J Am Chem Soc* 128:1808–1809. doi:  
39 10.1021/ja0577692  
40  
41  
42  
43  
44  
45  
46  
47  
48  
49  
50  
51  
52  
53  
54  
55  
56  
57  
58  
59  
60

- 1  
2  
3 9. Phillips RM, Bair E, Lawrence DS, Sims CE, Allbritton NL (2013) Measurement of protein  
4 tyrosine phosphatase activity in single cells by capillary electrophoresis. *Anal Chem*  
5  
6 85:6136–6142. doi: 10.1021/ac401106e  
7  
8
- 9  
10 10. Turner AH, Lebhar MS, Proctor A, Wang Q, Lawrence DS, Allbritton NL (2016) Rational  
11 Design of a Dephosphorylation-Resistant Reporter Enables Single-Cell Measurement of  
12 Tyrosine Kinase Activity. *ACS Chem Biol* 11:355–362. doi: 10.1021/acscchembio.5b00667  
13  
14
- 15 11. Rehm M, Dussmann H, Janicke RU, Tavare JM, Kogel D, Prehn JHM (2002) Single-cell  
16 fluorescence resonance energy transfer analysis demonstrates that caspase activation during  
17 apoptosis is a rapid process. Role of caspase-3. *J Biol Chem* 277:24506–24514. doi:  
18  
19 10.1074/jbc.M110789200  
20  
21
- 22 12. Ni Q, Titov DV, Zhang J (2006) Analyzing protein kinase dynamics in living cells with  
23 FRET reporters. *Methods* 40:279–286. doi: 10.1016/j.ymeth.2006.06.013  
24  
25
- 26 13. Ng EX, Miller MA, Jing T, Chen C-H (2016) Single cell multiplexed assay for proteolytic  
27 activity using droplet microfluidics. *Biosensors and Bioelectronics* 81:408–414. doi:  
28  
29 10.1016/j.bios.2016.03.002  
30  
31
- 32 14. Lee CL, Linton J, Soughayer JS, Sims CE, Allbritton NL (1999) Localized measurement of  
33 kinase activation in oocytes of *Xenopus laevis*. *Nat Biotechnol* 17:759–762. doi:  
34  
35 10.1038/11691  
36  
37
- 38 15. Bozinovski S, Cristiano BE, Marmy-Conus N, Pearson RB (2002) The Synthetic Peptide  
39 RPRAAATF Allows Specific Assay of Akt Activity in Cell Lysates. *Analytical Biochemistry*  
40  
41 305:32–39. doi: 10.1006/abio.2002.5659  
42  
43  
44  
45  
46  
47  
48  
49  
50  
51  
52  
53  
54  
55  
56  
57  
58  
59  
60

- 1  
2  
3  
4  
5  
6  
7  
8  
9  
10  
11  
12  
13  
14  
15  
16  
17  
18  
19  
20  
21  
22  
23  
24  
25  
26  
27  
28  
29  
30  
31  
32  
33  
34  
35  
36  
37  
38  
39  
40  
41  
42  
43  
44  
45  
46  
47  
48  
49  
50  
51  
52  
53  
54  
55  
56  
57  
58  
59  
60
16. Proctor A, Wang Q, Lawrence DS, Allbritton NL (2012) Development of a peptidase-resistant substrate for single-cell measurement of protein kinase B activation. *Anal Chem* 84:7195–7202. doi: 10.1021/ac301489d
17. Tung CH, Mahmood U, Bredow S, Weissleder R (2000) In vivo imaging of proteolytic enzyme activity using a novel molecular reporter. *Cancer Res* 60:4953–4958.
18. Dragulescu-Andrasi A, Liang G, Rao J (2009) In vivo bioluminescence imaging of furin activity in breast cancer cells using bioluminogenic substrates. *Bioconjug Chem* 20:1660–1666. doi: 10.1021/bc9002508
19. Brown RB, Hewel JA, Emili A, Audet J (2010) Single amino acid resolution of proteolytic fragments generated in individual cells. *Cytometry A* 77:347–355. doi: 10.1002/cyto.a.20880
20. Yewdell JW, Reits E, Neefjes J (2003) Making sense of mass destruction: quantitating MHC class I antigen presentation. *Nat Rev Immunol* 3:952–961. doi: 10.1038/nri1250
21. Proctor A, Wang Q, Lawrence DS, Allbritton NL (2012) Metabolism of Peptide Reporters in Cell Lysates and Single Cells. *Analyst* 137:3028–3038. doi: 10.1039/c2an16162a
22. Reits E, Griekspoor A, Neijssen J, Groothuis T, Jalink K, van Veelen P, Janssen H, Calafat J, Drijfhout JW, Neefjes J (2003) Peptide diffusion, protection, and degradation in nuclear and cytoplasmic compartments before antigen presentation by MHC class I. *Immunity* 18:97–108.
23. Yang S, Proctor A, Cline LL, Houston KM, Waters ML, Allbritton NL (2013)  $\beta$ -Turn sequences promote stability of peptide substrates for kinases within the cytosolic environment. *The Analyst* 138:4305. doi: 10.1039/c3an00874f



- 1  
2  
3 24. Gladfelter AS (2015) How nontraditional model systems can save us. *Mol Biol Cell*  
4 26:3687–3689. doi: 10.1091/mbc.E15-06-0429  
5  
6
- 7  
8 25. Page MJ, Di Cera E (2008) Evolution of Peptidase Diversity. *Journal of Biological*  
9 *Chemistry* 283:30010–30014. doi: 10.1074/jbc.M804650200  
10  
11
- 12 26. Tamura Y, Niinobe M, Arima T, Okuda H, Fujii S (1975) Aminopeptidases and  
13 arylamidases in normal and cancer tissues in humans. *Cancer Res* 35:1030–1034.  
14  
15
- 16 27. Mainz ER, Serafin DS, Nguyen TT, Tarrant TK, Sims CE, Allbritton NL (2016) Single Cell  
17 *Chemical Cytometry of Akt Activity in Rheumatoid Arthritis and Normal Fibroblast-like*  
18 *Synoviocytes in Response to Tumor Necrosis Factor  $\alpha$ . Analytical Chemistry.* doi:  
19 10.1021/acs.analchem.6b01801  
20  
21
- 22 28. Fey P, Dodson RJ, Basu S, Chisholm RL (2013) One stop shop for everything  
23 *Dictyostelium: dictyBase and the Dicty Stock Center in 2012.* In: Eichinger L, Rivero F  
24 (eds) *Dictyostelium discoideum Protocols.* Humana Press, pp 59–92  
25  
26
- 27 29. Fey P, Kowal AS, Gaudet P, Pilcher KE, Chisholm RL (2007) Protocols for growth and  
28 *development of Dictyostelium discoideum.* *Nat Protoc* 2:1307–1316. doi:  
29 10.1038/nprot.2007.178  
30  
31
- 32 30. De Bernardo S, Weigele M, Toome V, Manhart K, Leimgruber W, Böhlen P, Stein S,  
33 Udenfriend S (1974) Studies on the reaction of fluorescamine with primary amines. *Arch*  
34 *Biochem Biophys* 163:390–399.  
35  
36
- 37 31. Kelley, CT (1999) *Iterative Methods for Optimization.* SIAM, Philadelphia  
38  
39
- 40 32. Alessi DR, Cohen P (1998) Mechanism of activation and function of protein kinase B.  
41 *Current Opinion in Genetics & Development* 8:55–62. doi: 10.1016/S0959-  
42 437X(98)80062-2  
43  
44  
45  
46  
47  
48  
49  
50  
51  
52  
53  
54  
55  
56  
57  
58  
59  
60

- 1  
2  
3  
4  
5  
6  
7  
8  
9  
10  
11  
12  
13  
14  
15  
16  
17  
18  
19  
20  
21  
22  
23  
24  
25  
26  
27  
28  
29  
30  
31  
32  
33  
34  
35  
36  
37  
38  
39  
40  
41  
42  
43  
44  
45  
46  
47  
48  
49  
50  
51  
52  
53  
54  
55  
56  
57  
58  
59  
60
33. Proctor A, Herrera-Loeza SG, Wang Q, Lawrence DS, Yeh JJ, Allbritton NL (2014) Measurement of protein kinase B activity in single primary human pancreatic cancer cells. *Anal Chem* 86:4573–4580. doi: 10.1021/ac500616q
  34. Fabrizio P, Pozza F, Pletcher SD, Gendron CM, Longo VD (2001) Regulation of longevity and stress resistance by Sch9 in yeast. *Science* 292:288–290. doi: 10.1126/science.1059497
  35. Meili R, Ellsworth C, Lee S, Reddy TB, Ma H, Firtel RA (1999) Chemoattractant-mediated transient activation and membrane localization of Akt/PKB is required for efficient chemotaxis to cAMP in *Dictyostelium*. *EMBO J* 18:2092–2105. doi: 10.1093/emboj/18.8.2092
  36. Anderson DH (2013) *Compartmental Modeling and Tracer Kinetics*. Springer Science & Business Media
  37. Guan S, Price JC, Ghaemmaghami S, Prusiner SB, Burlingame AL (2012) Compartment Modeling for Mammalian Protein Turnover Studies by Stable Isotope Metabolic Labeling. *Anal Chem* 84:4014–4021. doi: 10.1021/ac203330z
  38. Kuzmic P (1996) Program DYNAFIT for the analysis of enzyme kinetic data: application to HIV proteinase. *Anal Biochem* 237:260–273. doi: 10.1006/abio.1996.0238
  39. Petretera A, Lai ZW, Schilling O (2014) Carboxyterminal Protein Processing in Health and Disease: Key Actors and Emerging Technologies. *Journal of Proteome Research* 13:4497–4504. doi: 10.1021/pr5005746
  40. Weimershaus M, Evnouchidou I, Saveanu L, van Endert P (2013) Peptidases trimming MHC class I ligands. *Curr Opin Immunol* 25:90–96. doi: 10.1016/j.coi.2012.10.001

- 1  
2  
3  
4  
5  
6  
7  
8  
9  
10  
11  
12  
13  
14  
15  
16  
17  
18  
19  
20  
21  
22  
23  
24  
25  
26  
27  
28  
29  
30  
31  
32  
33  
34  
35  
36  
37  
38  
39  
40  
41  
42  
43  
44  
45  
46  
47  
48  
49  
50  
51  
52  
53  
54  
55  
56  
57  
58  
59  
60
41. Milo R, Jorgensen P, Moran U, Weber G, Springer M (2010) BioNumbers—the database of key numbers in molecular and cell biology. *Nucleic Acids Res* 38:D750–D753. doi: 10.1093/nar/gkp889
  42. Rawlings ND (2009) A large and accurate collection of peptidase cleavages in the MEROPS database. *Database (Oxford)* 2009:bap015. doi: 10.1093/database/bap015
  43. Rawlings ND, Barrett AJ, Finn R (2016) Twenty years of the MEROPS database of proteolytic enzymes, their substrates and inhibitors. *Nucleic Acids Res* 44:D343–350. doi: 10.1093/nar/gkv1118
  44. Cousin C, Derouiche A, Shi L, Pagot Y, Poncet S, Mijakovic I (2013) Protein-serine/threonine/tyrosine kinases in bacterial signaling and regulation. *FEMS Microbiology Letters* 346:11–19. doi: 10.1111/1574-6968.12189
  45. Krachler AM, Woolery AR, Orth K (2011) Manipulation of kinase signaling by bacterial pathogens. *J Cell Biol* 195:1083–1092. doi: 10.1083/jcb.201107132

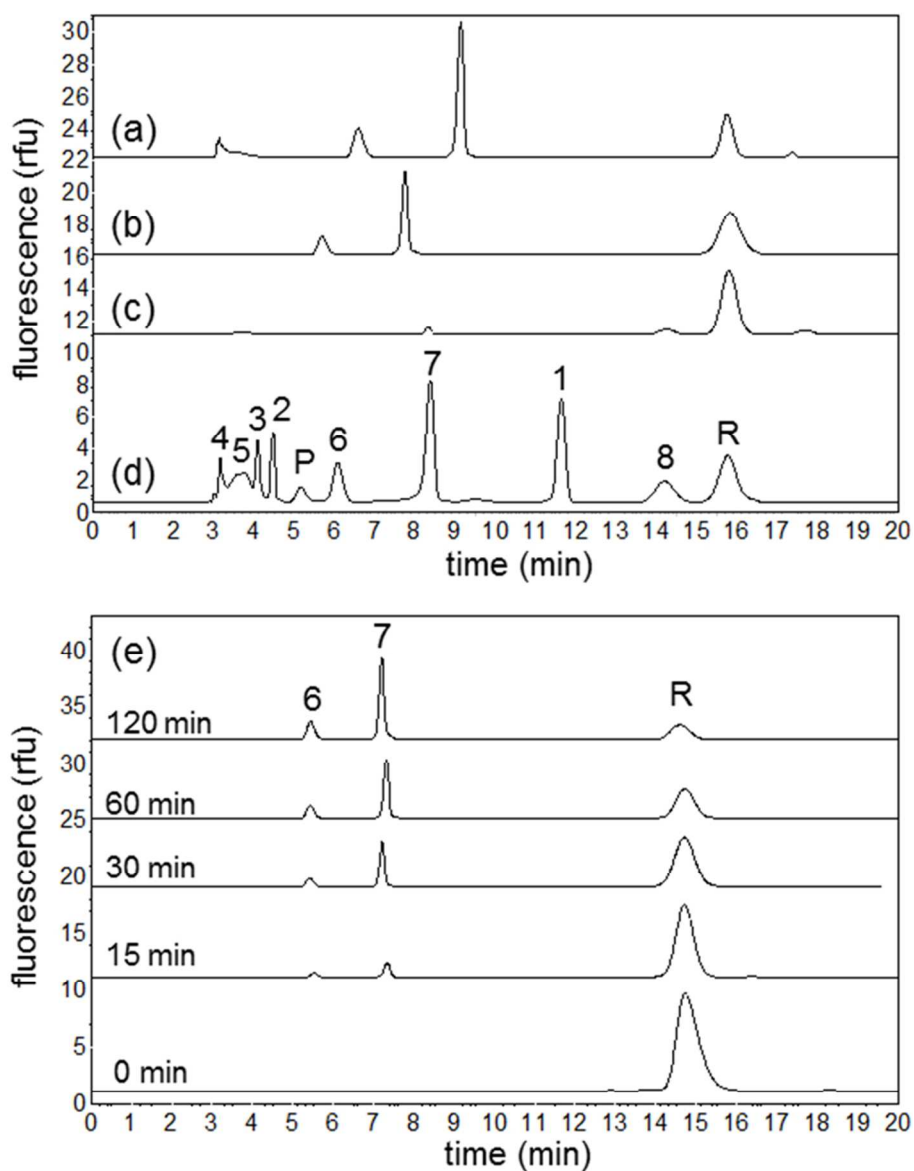


**Fig. 1** Capillary electropherograms of peptide samples incubated for 60 min in cell lysates prepared from (a) *E. coli*, (b) *D. discoideum*, and (c) *S. cerevisiae*, and (d) of peptide standards. *R* represents the unmodified, full-length reporter, *P* is the phosphorylated reporter, and 1-8 represent N-terminal fluorescent fragments of the reporter (referred to as  $F_1$ - $F_8$  in the text). For display only, the time axes of all electropherograms were normalized to the migration times for the parent reporter (*R*) and the five amino acid fragment to facilitate comparisons. (e) Capillary electropherograms for reporter incubated in *D. discoideum* cell lysate for 0 min to 120 min showing degradation of the reporter and formation of fragments over time.

82x106mm (300 x 300 DPI)

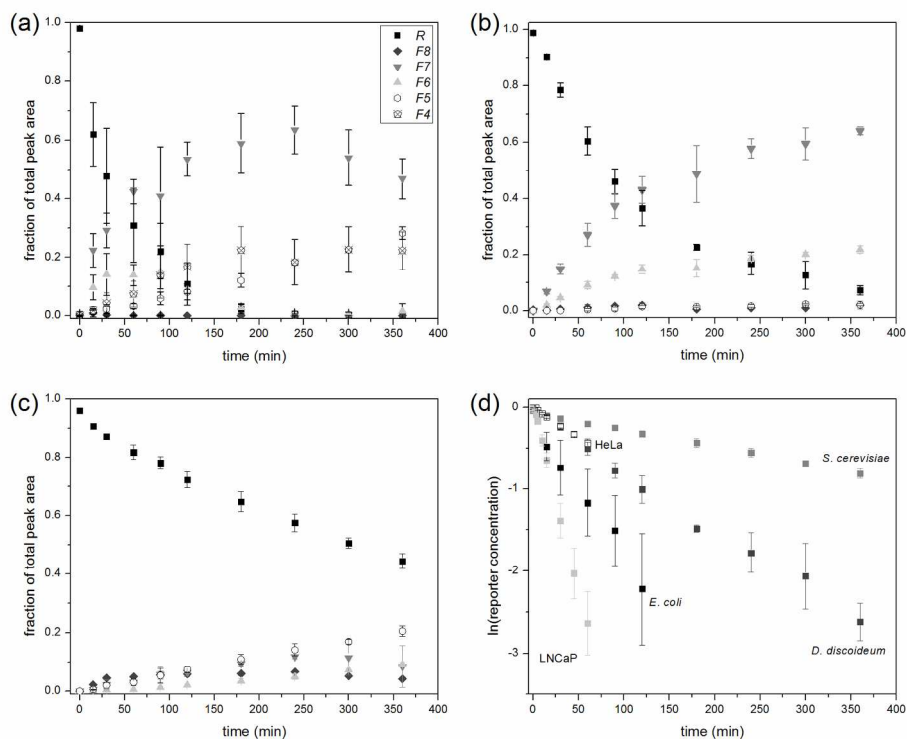


**Fig. 2** Peptide abundances as a function of time for metabolism of the reporter in lysates from (a) *E. coli*, (b) *D. discoideum*, and (c) *S. cerevisiae*. Data points are average values for  $n = 3$  biological replicates; error bars show the standard deviation. (d) Linearized semi-log plots of the abundance of full-length reporter (*R*) as a function of time. The slope of each line gives the first-order rate constant for overall degradation of the reporter ( $k_{\text{net}, R}$ ). Data for HeLa and LNCaP cells are from ref. [16].

173x137mm (300 x 300 DPI)

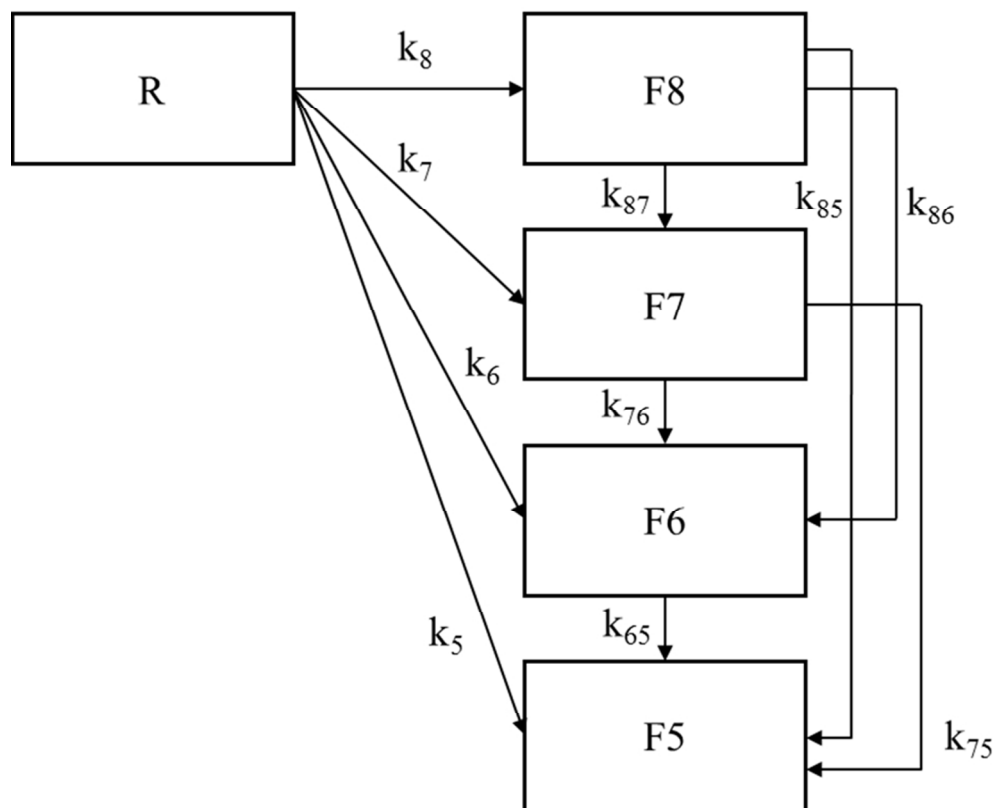


**Fig. 3** Compartment-based model of reporter ( $R$ ) metabolism into shorter N-terminal fragments ( $F_x$ ) with  $X$  remaining amino acid residues after the N-terminal fluorescent label. The kinetics of each reaction are described as a rate constant,  $k$ .

82x66mm (300 x 300 DPI)

**Table 1** Rate constants for peptidase reactions of the reporter in each species, as determined by compartment-based models. Unreported values (--) indicate that one of the fragments involved in the reaction was not observed experimentally and therefore not included in the model. For example,  $R_4$  was not observed in any experiments except those conducted with *E. coli*.

Rate Constant ( $\text{min}^{-1}$ )	<i>E. coli</i>	<i>D. discoideum</i>	<i>S. cerevisiae</i>	HeLa	LNCap
$k_8$	--	$2 \times 10^{-4}$	$2 \times 10^{-3}$	$3 \times 10^{-3}$	$5 \times 10^{-3}$
$k_7$	$1 \times 10^{-2}$	$5 \times 10^{-3}$	$2 \times 10^{-4}$	$2 \times 10^{-4}$	$5 \times 10^{-4}$
$k_6$	$9 \times 10^{-3}$	$2 \times 10^{-3}$	$2 \times 10^{-14}$	$2 \times 10^{-4}$	$2 \times 10^{-2}$
$k_5$	$8 \times 10^{-8}$	$2 \times 10^{-4}$	$6 \times 10^{-4}$	$4 \times 10^{-3}$	$2 \times 10^{-2}$
$k_4$	$2 \times 10^{-14}$	--	--	--	--
$k_{net,R}$	$2 \times 10^{-2}$	$7 \times 10^{-3}$	$2 \times 10^{-3}$	$7 \times 10^{-3}$	$4 \times 10^{-2}$
$k_{87}$	--	$1 \times 10^{-13}$	$2 \times 10^{-2}$	$2 \times 10^{-2}$	$5 \times 10^{-2}$
$k_{86}$	--	$4 \times 10^{-3}$	$4 \times 10^{-8}$	$1 \times 10^{-11}$	$1 \times 10^{-14}$
$k_{85}$	--	$2 \times 10^{-14}$	$2 \times 10^{-14}$	$2 \times 10^{-2}$	$1 \times 10^{-2}$
$k_{84}$	--	--	--	--	--
$k_{net,8}$	--	$4 \times 10^{-3}$	$2 \times 10^{-2}$	$4 \times 10^{-2}$	$7 \times 10^{-2}$
$k_{76}$	$3 \times 10^{-6}$	$2 \times 10^{-11}$	$5 \times 10^{-3}$	$3 \times 10^{-2}$	$2 \times 10^{-14}$
$k_{75}$	$4 \times 10^{-4}$	$4 \times 10^{-4}$	$4 \times 10^{-3}$	$1 \times 10^{-3}$	$1 \times 10^{-1}$
$k_{74}$	$2 \times 10^{-14}$	--	--	--	--
$k_{net,7}$	$4 \times 10^{-4}$	$4 \times 10^{-4}$	$1 \times 10^{-2}$	$3 \times 10^{-2}$	$1 \times 10^{-1}$
$k_{65}$	$2 \times 10^{-14}$	$3 \times 10^{-12}$	$2 \times 10^{-9}$	$1 \times 10^{-2}$	1 *
$k_{64}$	$2 \times 10^{-2}$	--	--	--	--
$k_{net,6}$	$2 \times 10^{-2}$	$3 \times 10^{-12}$	$2 \times 10^{-9}$	$1 \times 10^{-2}$	1 *
$k_{54} = k_{net,5}$	$5 \times 10^{-13}$	--	--	--	--

\*Upper bound of allowed values.

**Table 2** Summary of kinetic data for reporter metabolism in each cell type. Ranges represent the 90% confidence interval for each value as determined by a bootstrapping method. The major fragments for HeLa and LNCaP lysates were determined in reference [16].

Cell Type	Half-Life (min)	Initial Rate (pmol mg <sup>-1</sup> s <sup>-1</sup> )	Major Fragment during First Hour
<i>E. coli</i>	21-44	0.09-0.18	6FAM-GRP(nR)AFT
<i>D. discoideum</i>	82-103	0.038-0.047	6FAM-GRP(nR)AFT
<i>S. cerevisiae</i>	279-314	0.012-0.014	6FAM-GRP(nR)AFTF
HeLa (human cervical cancer)	86-105	0.037-0.045	6FAM-GRP(nR)A
LNCaP (human prostate cancer)	13-18	0.22-0.30	6FAM-GRP(nR)A



## Electronic Supplemental Material

### Interspecies Comparison of Peptide Substrate Reporter Metabolism using Compartment-Based Modeling

Allison J. Tierney,<sup>a</sup> Nhat Pham,<sup>b</sup> Kunwei Yang,<sup>a</sup> Brooks K. Emerick,<sup>b</sup> and Michelle L. Kovarik<sup>a,\*</sup>

<sup>a</sup>Department of Chemistry, Trinity College, 300 Summit Street, Hartford, CT 06106

<sup>b</sup>Department of Mathematics, Trinity College, 300 Summit Street, Hartford, CT 06106

\*Corresponding Author. Email: michelle.kovarik@trincoll.edu. Phone: 860-297-5275. Fax: 860-297-5129

#### Compartment-Based Model for *E. coli*

In lysates from eukaryotic cells (*D. discoideum*, *S. cerevisiae*, HeLa, and LNCaP) we detected fragments  $F_8$  through  $F_5$ . In *E. coli* lysates, we observed fragments  $F_7$  to  $F_4$ . As a result, a slightly different compartment-based model was required to describe this system (Fig. S1). This model is mathematically equivalent to the model in Fig. 3 of the article (used to describe data for the eukaryotic cells), and the same assumptions were applied. Namely, (1) there is no source of peptide fragments except for the initial reporter; (2) the parent peptide or any smaller fragments do not leave the system, but are simply converted to smaller fragments; (3) any larger peptide could be cleaved to form any smaller peptide, but only the N-terminal fragments, which retain the 6-FAM label, will be detected and (4) a linear system of equations is created, given that the system follows first-order kinetics and all rate constants are non-negative.

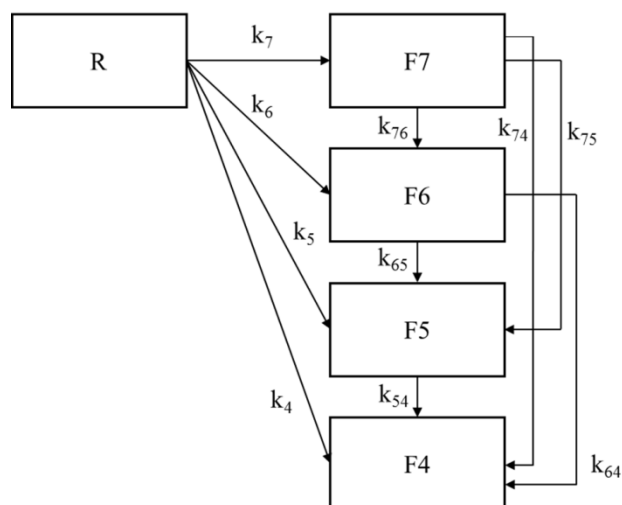


**Fig. S1.** Compartment-based model of reporter ( $R$ ) metabolism into shorter N-terminal fragments ( $F_X$ ) with  $X$  remaining amino acid residues after the N-terminal fluorescent label for *E. coli*.

## Simplified Model for LNCaP

$F_6$  (the six amino acid fragment) was not observed in LNCaP lysates. This observation could be explained either of two ways:  $F_6$  formed but was rapidly degraded to  $F_5$  or  $F_6$  was never formed. Results from the original model for eukaryotic cells (Fig. 3) suggested that  $F_6$  formed but was rapidly degraded. To further test this hypothesis, we constructed an alternate, simplified model (Fig. S2) in which  $F_6$  never formed.

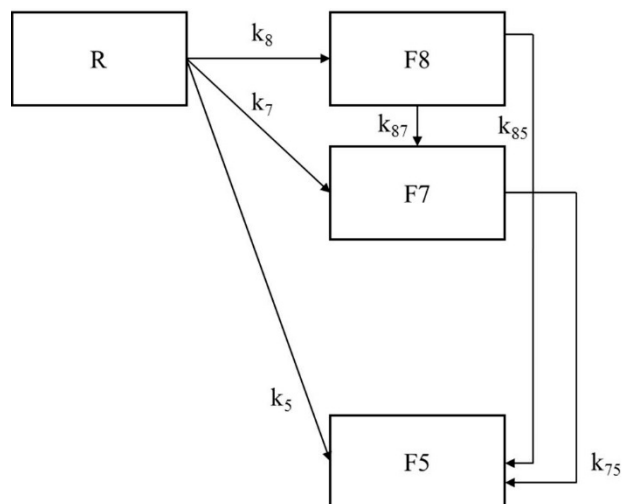


**Fig. S2.** Simplified compartment-based model of reporter ( $R$ ) metabolism in LNCaP lysates, assuming that  $F_6$  was never detected because it never formed.

## Data Fitting

To fit our model to the data, we first solved the linear system that describes the compartment based model. Equations (1)-(5) found in the article and reproduced below represent the model in Fig. 3. An analogous series of equations was written and solved for the *E. coli* model in Fig. S1.

$$\frac{dR}{dt} = -(k_8 + k_7 + k_6 + k_5)R = -k_{net,R}R \quad (1)$$

$$\frac{dF_8}{dt} = -(k_{87} + k_{86} + k_{85})F_8 + k_8R = -k_{net,8}F_8 + k_8R \quad (2)$$

$$\frac{dF_7}{dt} = -(k_{76} + k_{75})F_7 + k_{87}F_8 + k_7R = -k_{net,7}F_7 + k_{87}F_8 + k_7R \quad (3)$$

$$\frac{dF_6}{dt} = -k_{65}F_6 + k_{76}F_7 + k_{86} + k_6R \quad (4)$$

$$\frac{dF_5}{dt} = k_{65}F_6 + k_{75}F_7 + k_{85}F_8 + k_5R \quad (5)$$

These solutions to these equations are found using basic techniques for solving differential equations and are shown in Equations (6)-(10):

$$R(t) = e^{-k_{net,R}t} \quad (6)$$

$$F_8(t) = \frac{k_8}{k_{net,R}-k_8} (e^{-k_{net,8}t} - e^{-k_{net,R}t}) \quad (7)$$

$$F_7(t) = \frac{k_{87}k_8(k_{net,7}-k_{net,R}) - (k_{87}k_8 + k_7k_{net,8} - k_7k_{net,R})(k_{net,7}-k_{net,8})}{(k_{net,8}-k_{net,R})(k_{net,7}-k_{net,R})} e^{-k_{net,7}t} + \frac{k_{87}k_8}{(k_{net,R}-k_{net,8})(k_{net,7}-k_{net,8})} + \frac{k_{87}k_8 + k_7(k_{net,8}-k_{net,R})}{(k_{net,8}-k_{net,R})(k_{net,7}-k_{net,R})} \quad (8)$$

$$F_6(t) = - \left[ \frac{k_{76}k_{87}k_8(k_{net,7}-k_{net,R}) + k_{76}(k_7k_8 - k_{87}k_8 - k_7k_{net,R})(k_{net,7}-k_{net,8})}{(k_{net,8}-k_{net,R})(k_{net,7}-k_{net,R})(k_{net,7}-k_{net,8})(k_{net,6}-k_{net,7})} + \frac{k_{76}k_{87}k_8 + k_{86}k_8(k_{net,7}-k_{net,8})}{(k_{net,6}-k_{net,8})(k_{net,7}-k_{net,8})(k_{net,R}-k_{net,8})} + \frac{k_{76}k_{87}k_8 + k_7k_6(k_{net,8}-k_{net,R}) + k_6k_8(k_{net,7}-k_{net,R}) + k_6(k_{net,8}-k_{net,R})(k_{net,7}-k_{net,R})}{(k_{net,8}-k_{net,R})(k_{net,7}-k_{net,R})(k_{net,6}-k_{net,R})} \right] e^{-k_{net,6}t} + \frac{k_{76}k_{87}k_8(k_{net,7}-k_{net,R}) + k_{76}(k_7k_8 - k_{87}k_8 - k_7k_{net,R})(k_{net,7}-k_{net,8})}{(k_{net,8}-k_{net,R})(k_{net,7}-k_{net,R})(k_{net,7}-k_{net,8})(k_{net,6}-k_{net,7})} e^{-k_{net,7}t} + \frac{k_{76}k_{87}k_8 + k_{86}k_8(k_{net,7}-k_{net,8})}{(k_{net,6}-k_{net,8})(k_{net,7}-k_{net,8})(k_{net,R}-k_{net,8})} e^{-k_{net,8}t} + \frac{k_{76}k_{87}k_8 + k_7k_6(k_{net,8}-k_{net,R}) + k_6k_8(k_{net,7}-k_{net,R}) + k_6(k_{net,8}-k_{net,R})(k_{net,7}-k_{net,R})}{(k_{net,8}-k_{net,R})(k_{net,7}-k_{net,R})(k_{net,6}-k_{net,R})} e^{-k_{net,R}t} \quad (9)$$

$$F_5(t) = 1 - R(t) - F_8(t) - F_7(t) - F_6(t) \quad (10)$$

We note that the function  $F_5(t)$  is completely determined by the previous four solutions; thus, the parameters  $k_{65}$ ,  $k_{75}$ ,  $k_{85}$  and  $k_5$  are determined after finding best fit values for  $k_{net,6}$ ,  $k_{net,7}$ ,  $k_{net,8}$ , and  $k_{net,R}$ . This leaves ten model parameters that we wish to fit to the experimental data points. We note here that the solution functions are written to show what parameters they depend on as well as the independent variable,  $t$ . For example, the function  $R(t)$  depends on the parameters  $k_{net,R}$ , so we write  $R(t, k_{net,R})$ .

The experiments yielded time-series data collected over the course of one or three hours (for human and non-human cell types, respectively) for the reporter and each N-terminal fragment of the reporter. The measurements were taken at ten different time points, and there were three measurements at each time point. We used the average of the three values for our data-fitting purposes and considered the standard deviation of these measurements for our Monte-Carlo simulations (see below). We found the best fit parameters for each segment by matching Equations (6)-(10) (i.e., the explicit solutions to Equations (1)-(5)) to the given time-series data in the least-squares sense. Because we quantified each fragment individually, we first found the best fit parameter for the parent peptide,  $R(t)$ , then found the best fit parameters for  $F_8(t)$ , and so on. Our method for fitting all ten parameters is summarized below.

### Fitting data for the reporter ( $R$ )

Given the data for the degradation of the reporter ( $R$ ), we found the parameter  $k_{\text{net,R}}$  using the least-squares data fitting approach with the function  $R(t; k_{\text{net,R}})$ . The function  $R(t; k_{\text{net,R}}) = e^{-k_{\text{net,R}}t}$  only has one parameter, namely  $k_{\text{net,R}}$ , the degradation rate of the reporter. We linearized the function by taking the natural logarithm,  $\ln(R) = -k_{\text{net,R}}t$ , and matched it to the logarithm of the given data. Using the least-squares regression line, we minimized the residual error and found the best fit for the parameter  $k_{\text{net,R}}$ .

### Fitting data for $F_8$

We substituted this best fit value for  $k_{\text{net,R}}$  into the solution for  $F_8$ , which means  $F_8$  is dependent on  $k_{\text{net,8}}$  and  $k_8$ . We fit the function  $F_8(t; k_{\text{net,8}}, k_8)$  to the data for  $F_8$ . Since the function  $F_8(t; k_{\text{net,8}}, k_8)$  cannot be linearized like the function  $R(t; k_{\text{net,R}})$ , we used a nonlinear least-squares approach. Assuming the error in measurements is taken from the standard normal curve, we defined the function

$$f_8(k_{\text{net,8}}, k_8) = \| F_8([\text{Time Data}]; k_{\text{net,8}}, k_8) - [F_8 \text{ Data}] \| \quad (11)$$

as the error function to be minimized. Here, [Time Data] represents the ten time points,  $[F_8 \text{ Data}]$  is the average measurements of  $F_8$  concentration at each of ten time points, and  $\| \cdot \|$  is the Euclidean norm. Using the MatLab lsqnonlin function, we ran the iterative method for each trial until a minimum was found in  $(k_{\text{net,8}}; k_8)$  parameter space and reported the best fit parameters, corresponding to the minimum residual error, in Table 1 in the article. We assume that the degradation constant,  $k_{\text{net,8}}$  is non-negative and bounded above by one. Further, to ensure that other parameters are non-negative, we bound the parameter  $k_8$  above by  $k_{\text{net,R}}$ . The reason for this is because we know  $k_{\text{net,R}} - k_8 = k_7 + k_6 + k_5 \geq 0$ , which implies  $k_{\text{net,R}} - k_8 \geq 0$  and hence  $k_8 \leq k_{\text{net,R}}$ . A similar argument can be made for the remainder of the parameters below.

### Fitting data for $F_7$

We substituted the best fit parameter values for  $k_{\text{net,8}}$  and  $k_8$  into Equation (8) for  $F_7$  to form the function  $F_7(t; k_{\text{net,7}}, k_{87}, k_7)$ . We defined the error function as

$$f_7(k_{\text{net,7}}, k_{87}, k_7) = \| F_7([\text{Time Data}]; k_{\text{net,7}}, k_{87}, k_7) - [F_7 \text{ Data}] \| \quad (12)$$

We used the nonlinear least-squares method to fit the data for  $F_7$  using 27,000 trials. To ensure all parameter values were non-negative, we let  $k_{\text{net,7}}$  be bounded above by 1,  $k_{87}$  was bounded above by  $k_{\text{net,8}}$ , and  $k_7$  was bounded above by  $k_{\text{net,R}} - k_8$ . All values were bounded below by 0.

### Fitting data for $F_6$ and $F_5$

We substituted the best fit parameter values for  $k_{\text{net,7}}$ ,  $k_{87}$ , and  $k_7$  into  $F_6$  and  $F_5$  to form the functions  $F_6(t; k_{\text{net,6}}, k_{86}, k_{76}, k_6)$  and  $F_5(t; k_{\text{net,6}}, k_{86}, k_{76}, k_6)$ . Therefore, to find the best parameters for  $k_{\text{net,6}}$ ,  $k_{86}$ ,  $k_{76}$  and  $k_6$ , we minimized the error between the functions  $F_6$  and  $F_5$  with the data given for the two fragments, respectively. We defined the following error function

$$f_{65}(k_{\text{net,6}}, k_{86}, k_{76}, k_7, k_6) = \left\| \begin{bmatrix} F_6(\text{Time Data}; k_{\text{net,6}}, k_{86}, k_{76}, k_6) \\ F_5(\text{Time Data}; k_{\text{net,6}}, k_{86}, k_{76}, k_6) \end{bmatrix} - \begin{bmatrix} F_6 \text{ Data} \\ F_5 \text{ Data} \end{bmatrix} \right\| \quad (13)$$

We used the nonlinear least-squares method to fit  $F_6$  and  $F_5$  using 50,625 trials. To ensure every parameter is non-negative, we constrain the parameters for  $F_6$  to a lower bound of zero and the following upper bounds:  $k_{\text{net},6}$  is bounded above by 1;  $k_{86}$  is bounded above by  $k_{\text{net},8} - k_{87}$ ;  $k_{76}$  is bounded above by  $k_{\text{net},7}$ ; and  $k_6$  is bounded above by  $k_{\text{net},R} - k_8 - k_7$ .

In each step of the data-fitting procedure above, we minimized the residual norm between our functions evaluated at the time data and the measured data of each peptide concentration. The minimum residuals for each of the parameters are given in Table S1.

**Table S1.** Minimum residuals from the fitting of Equations (6)-(10) to the experimental data for each peptide and species.

	<i>E. coli</i>	<i>D. discoideum</i>	<i>S. cerevisiae</i>	HeLa	LNCap	LNCaP simplified
$R$	$1.47 \times 10^{-1}$	$9.32 \times 10^{-2}$	$1.16 \times 10^{-1}$	$2.10 \times 10^{-2}$	$7.94 \times 10^{-2}$	$7.94 \times 10^{-2}$
$F_8$	--	$2.77 \times 10^{-4}$	$3.02 \times 10^{-4}$	$9.75 \times 10^{-5}$	$3.21 \times 10^{-5}$	$3.21 \times 10^{-5}$
$F_7$	$2.36 \times 10^{-2}$	$2.30 \times 10^{-3}$	$6.90 \times 10^{-4}$	$6.53 \times 10^{-6}$	$1.13 \times 10^{-5}$	$4.36 \times 10^{-3}$
$F_6$	$1.29 \times 10^{-3}$	$4.24 \times 10^{-3}$	$1.69 \times 10^{-2}$	$2.24 \times 10^{-4}$	$4.63 \times 10^{-3}$	--
$F_5$	$1.98 \times 10^{-1}$					$4.36 \times 10^{-3}$
$F_4$		--	--	--	--	--

Given only ten data points for each peptide, we found it more economical to fit the data in a sequential order rather than all at the same time. In this way, we searched a much smaller parameter space in each step of the process. We compared both methods, and the sequential method described above yielded smaller residual norms. The nonlinear least-squares method requires an initial condition, and we found that different initial conditions sometimes yielded different best-fit parameters. To deal with this, we ran the same simulation with thousands of different initial conditions and chose the best-fit parameter to be the parameter set that yielded the minimum residual error among all trials. These values are given for each organism in Table 1 in the article. We compared the best-fit value to the most frequent value and concluded that generally they are very close in value within at least in order of magnitude. In cases where the best-fit value differs from the most frequent value, the error function likely has a broad local minimum that corresponds to the most frequent value and a sharper, deeper global minimum corresponding to the best-fit value. In this situation, most initial conditions will terminate to the broad, local minimum even though a better fit is obtained at the deeper global minimum. For this reason, we report values of  $k$  (Table 1) that correspond to the lowest minimum residuals (Table S1), even when they were not among the most frequently found parameter values.

### Bootstrapping

We considered the error in each measurement to create a confidence interval for the degradation constant for the full-length reporter,  $k_{\text{net},R}$ , for each organism. Each assay was repeated in triplicate, so for each time point,  $t$ , we had an average reporter concentration ( $\bar{R}$ ) and standard

deviation ( $s$ ) based on the three measurements. We assumed each measurement was a random variable that followed a Normal distribution with mean,  $\bar{R}$  and standard deviation,  $s$ . Using a Monte Carlo simulation, we generated a new, hypothetical data point called  $\hat{R}$ , at each time value,  $t$ , from the Normal distribution  $N(\bar{R}, t)$ . We constrained the hypothetical data points such that values below the limit of quantitation were assigned a value of zero and the maximum value was 1 since peptide concentrations were reported as fraction of total peak area. We generated 1000 data sets based on these criteria and fit the function  $R(t) = e^{k_{\text{net,R}}t}$  to each data set as described above. From this, we obtained histograms for the best fit parameter  $k_{\text{net,R}}$  from which we gain a confidence interval on our best fit value for  $k_{\text{net,R}}$  (Table S2). This essentially allows us to provide an idea of how the error in our measurements effects the confidence in our best fit values for the reporter degradation constant.

**Table S2.** Bootstrapped 90% confidence intervals for  $k_{\text{net,R}}$ .

	$k_{\text{net,R}}$ ( $\text{min}^{-1}$ )	
<i>E. coli</i>	$1.57 \times 10^{-2}$	- $3.33 \times 10^{-2}$
<i>D. discoideum</i>	$6.76 \times 10^{-3}$	- $8.49 \times 10^{-3}$
<i>S. cerevisiae</i>	$2.20 \times 10^{-3}$	- $2.48 \times 10^{-3}$
HeLa	$6.60 \times 10^{-3}$	- $8.07 \times 10^{-3}$
LNCaP	$3.94 \times 10^{-2}$	- $5.38 \times 10^{-2}$

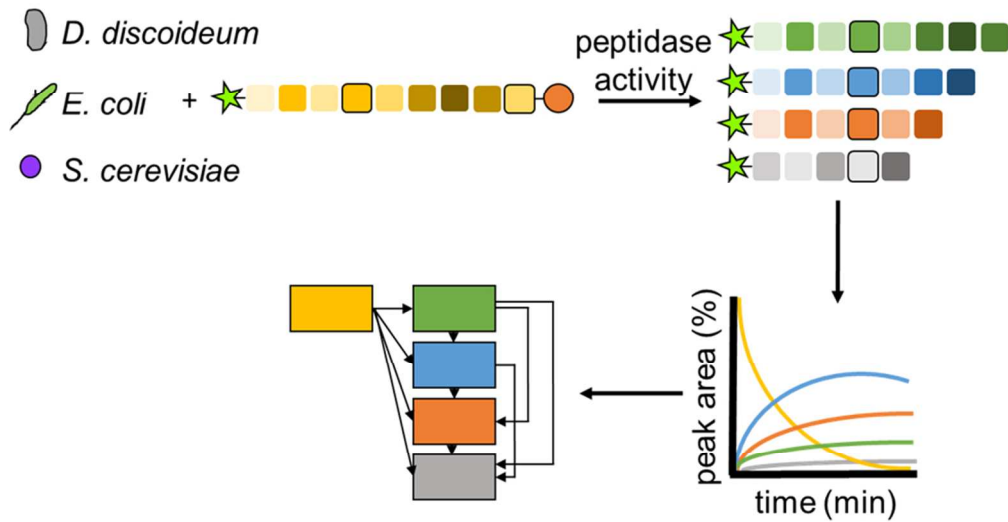
### Reporter Degradation and *D. discoideum* Social Development

To determine whether the reporter was metabolized differently in *D. discoideum* cells undergoing social development, we prepared lysates using the procedure described in the main article from cells that had been resuspended in development buffer (DB; 5 mM  $\text{Na}_2\text{HPO}_4$ , 5 mM  $\text{KH}_2\text{PO}_4$ , 1mM  $\text{CaCl}_2$  and 2mM  $\text{MgCl}_2$ ) at a density of  $10^7$  cells/mL for 2, 4, or 6 h. In this cell-dense, nutrient-free environment, *D. discoideum* cells begin gene expression for the initial stages of their social life cycle.

**Table S3.** Summary of kinetic data for VI-B metabolism in each cell type. Ranges represent the 90% confidence interval for each value as determined by the bootstrapping method described above.

Development Time (h)	Half-Life (min)	Initial Rate ( $\text{pmol mg}^{-1} \text{s}^{-1}$ )	Major Fragment during First Hour
0	82-103	0.038-0.047	6FAM-GRP(nR)AFT
2	79-89	0.043-0.049	6FAM-GRP(nR)AFT
4	83-92	0.042-0.047	6FAM-GRP(nR)AFT
6	94-110	0.035-0.041	6FAM-GRP(nR)AFT

Minimum residuals for  $k_{\text{net,R}}$  for the 2, 4, and 6 h development times were  $5.3 \times 10^{-2}$ ,  $8.6 \times 10^{-2}$ , and  $1.4 \times 10^{-1}$ , respectively.



Graphical Abstract

82x44mm (300 x 300 DPI)

1  
2  
3  
4  
5  
6  
7  
8  
9  
10  
11  
12  
13  
14  
15  
16  
17  
18  
19  
20  
21  
22  
23  
24  
25  
26  
27  
28  
29  
30  
31  
32  
33  
34  
35  
36  
37  
38  
39  
40  
41  
42  
43  
44  
45  
46  
47  
48  
49  
50  
51  
52  
53  
54  
55  
56  
57  
58  
59  
60